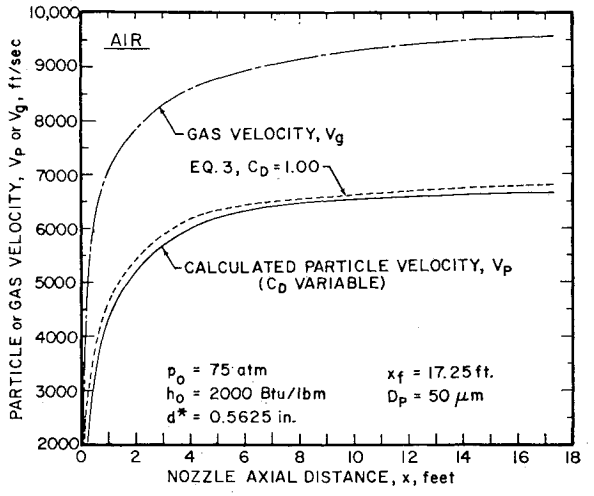


**Fig. 2 Comparison of approximate solution in Eq. (3) to a numerical solution for particle velocity along a conical shaped nozzle.**

tends to keep the gas density high for a longer time in the nozzle.

To test the accuracy of the approximate solution given in Eq. (3), a comparison with a numerical solution is shown in Fig. 2 where the real nozzle was approximated by a conical nozzle and the gas velocity at the end of each integration step was used in the solution. The agreement is seen to be good except in the nozzle throat region where the rapidly changing gas velocity deviates from the constant gas velocity asumption. In addition, the curves in Fig. 1 were used to evaluate the particle velocity along the nozzle and $V_{pi}$ was neglected in those curves. Using the same flow conditions and nozzle geometry given in Fig. 2, the effect of particle size on final particle velocity was computed and the results are shown in Fig. 3. Again the agreement between the approximate

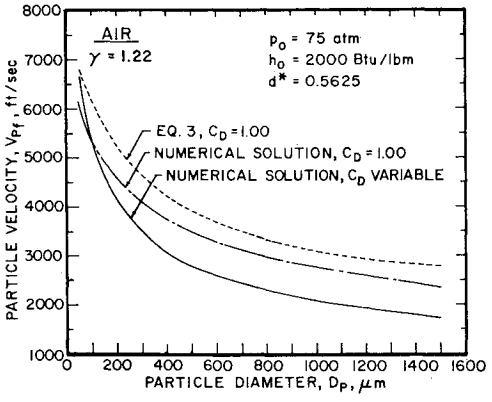


**Fig. 3 Effect of particle size on final particle velocity for conditions in Fig. 2.**

solution and the exact numerical solution is good with some deviation at the large particle size. All the approximate solutions were carried out with $C_D = 1.0$ which accounts for some of the errors at the large particle sizes. Since, for the larger Reynolds numbers associated with the larger particles $C_D$ decreases below one, computer solutions were carried out for $C_D = 1.0$ and compared with the approximate solution. The agreement is seen to be much better.

### Reference

[1] Lorenz, G. C., "Simulation of the Erosive Effects of Multiple Particle Impacts in Hypersonic Flow," *Journal of Spacecraft and Rockets*, Vol. 7, No. 2, Feb. 1970, pp. 119–125.

# Prediction of Pressure during Evacuation of Multilayer Insulation

A. P. M. GLASSFORD*
*Lockheed Palo Alto Research Laboratory, Palo Alto, Calif.*

### Nomenclature

| | |
|---|---|
| $c$ | = constant in Eq. (10) |
| $f$ | = specular reflection coefficient |
| $k$ | = constant in Eq. (10) |
| $L$ | = evacuation flow length |
| $M$ | = molecular weight |
| $P$ | = gas pressure |
| $Q$ | = outgassing rate |
| $R_0$ | = universal gas constant |
| $T$ | = temperature |
| $v_a$ | = mean molecular velocity |
| $v_0$ | = gas flow velocity at channel wall |
| $v_x, \bar{v}_x$ | = gas flow, mean gas flow velocity |
| $x,y,z$ | = coordinate system defined in Fig. 1 |
| $y_0$ | = half interlayer separation distance |
| $\mu$ | = gas viscosity |
| $\rho$ | = gas density |
| $\varepsilon$ | = shear stress proportionability constant |
| $\tau$ | = gas flow shear stress |
| $\zeta$ | = slip coefficient |
| $\varphi_{pd}, \varphi_{dp}$ | = parameters defined by Eqs. (3) and (4) |

*Subscripts*

| | |
|---|---|
| $p$ | = purge gas |
| $d$ | = desorbed gas |
| $m$ | = gas mixture |

### Introduction

MULTILAYER insulation systems require that the interlayer gas pressure be below about $10^{-4}$ torr for full insulative effectiveness to be achieved. Below this pressure thermal conduction through the residual gas is negligible in comparison with radiation and solid contact conduction. In space applications the interlayer gas pressure must be reduced from one atmosphere to this operational figure by auxiliary pumping equipment, or by evacuation to the atmosphere during ascent. In some applications it may be necessary to pressurize and re-evacuate the multilayers repeatedly in the course of successive missions. This paper describes an improved analytical procedure for predicting the insulation pressure history.

Previous analyses[1,2] of the evacuation of multilayer insulation systems have assumed a parallel plate isothermal flow model with constant interlayer separation, and have treated flow in the laminar continuum and free molecule regimes separately. Outgassing has not been included, and the gas flow has been assumed to be single component. The analysis presented in this paper uses the same simple geometric model but improves the representation of the gas flow by developing simultaneous flow equations for more than one gas component which include the effect of outgassing and

Received November 1, 1971; revision received January 5, 1972. Development of the analytical method was sponsored by the Lockheed Missile and Space Company. The experimental data presented were obtained under contract NAS 8-20758, NASA Marshall Space Flight Center, under the direction of E. Haskell Hyde. The numerical solution to the flow equations was programmed initially for the TYMSHARE System by Shirley L. McDonald and finally for the UNIVAC 1108 by Danielle J. Colvin.

Index categories: Fuel and Propellant Storage, Transfer and Control Systems; Launch Vehicle or Missile Simulation; Thermal Modeling and Experimental Thermal Simulation.

* Research Scientist, Engineering Sciences Laboratory.

which are valid for all flow regimes. The utility of the analytical procedure is demonstrated by comparing the analytical prediction with the results of a specific insulation evacuation laboratory experiment.

### *Derivation of the flow equations*

The model for the flow analysis is shown in Fig. 1. The multilayers are assumed to be flat plates of infinite length in the $z$ direction. The ratio of interlayer height $2y_0$ to width $2L$ is assumed to be negligibly small. Flow occurs solely in the positive and negative $x$ directions and there is a no-flow $y-z$ plane at $x=0$. The flow resistance between the edge of the sheets and the environment is assumed to be negligible. The gas between the multilayers is assumed to be a two-component mixture of the original purge gas and a single desorbed gas. The analysis is readily extensible to more than two components. Both gases are assumed to be perfect and the mixture is assumed to behave as a homogeneous gas whose molecular weight, $M_m$, viscosity, $\mu_m$,[3] and pressure $P_m$ are found as follows

$$M_m = (M_p P_p + M_d P_d)/(P_p + P_d) \tag{1}$$

$$\mu_m = \frac{\mu_p}{1 + (P_d/P_p)\varphi_{pd}} + \frac{\mu_d}{1 + (P_p/P_d)\varphi_{dp}} \tag{2}$$

where

$$\varphi_{pd} = [1 + (\mu_p/\mu_d)^{0.5}(M_d/M_p)^{0.25}]^2/[(2)^{1.5}(1 + M_p/M_d)^{0.5}] \tag{3}$$

$$\varphi_{dp} = [1 + (\mu_d/\mu_p)^{0.5}(M_p/M_d)^{0.25}]^2/[(2)^{1.5}(1 + M_d/M_p)^{0.5}] \tag{4}$$

$$P_m = P_p + P_d \tag{5}$$

Using these properties in a slip-flow modified flow analysis a single expression can be derived for the mean flow velocity of the mixture $\bar{v}_{xm}$ which is valid in the continuum transition and free molecule flow regimes. An analysis for flow between parallel plates is presented in the Appendix; it is similar to a previous analysis (Ref. 4, pp. 281–290) for flow in round tubes. The following expression is obtained for $\bar{v}_{xm}$ by writing Eq. (A10) in terms of mixture properties.

$$\bar{v}_{xm} = \frac{-{y_0}^2}{3\mu_m}\left[1 + \frac{4\mu_m v_{am}}{P_m y_0}\right]\frac{\partial P_m}{\partial x} \tag{6}$$

Continuity equations can then be written for each gas for flow through a volume element $2y_0 \cdot dx \cdot dz$.

For the desorbed gas:

$$\frac{\partial \rho_d}{\partial t} \cdot (2y_0 \cdot dx \cdot dz) = -\frac{\partial}{dx}(v_{xm} \cdot \rho_d) \cdot (2y_0 \cdot dx \cdot dz) + Q(2dx \cdot dz) \tag{7}$$

Equation (7) can be reduced to

$$\frac{\partial P_d}{\partial t} = -\bar{v}_{xm} \cdot \frac{\partial P_d}{\partial x} - P_d \cdot \frac{\partial \bar{v}_{xm}}{\partial x} + \frac{Q \cdot R_0 \cdot T}{y_0 M_d} \tag{8}$$

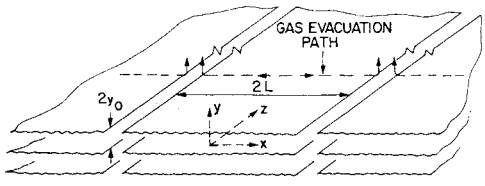


**Fig. 1 The idealized multilayer insulation geometric model used in the flow analysis.**

Similarly, for the purge gas

$$\frac{\partial P_p}{\partial t} = -\bar{v}_{xm} \cdot \frac{\partial P_p}{\partial x} - P_p \cdot \frac{\partial v_{xm}}{\partial x} \tag{9}$$

Equations (6, 8, and 9) are the flow equations which must be solved simultaneously to obtain the pressures $P_p$, $P_d$ and $P_m$ as functions of time. However, before a solution can be obtained the outgassing rate $Q$ must be specified.

Outgassing is the process by which the sorption concentration of a gas or in a solid adjusts from one equilibrium value to another equilibrium value. Sorption concentration is a function of the particular solid and its previous manufacturing and storage history, the solid geometry and temperature and gas pressure and temperature. Outgassing rate is a function of all these parameters plus time. Its magnitude cannot be predicted analytically with the accuracy required for engineering analysis and so experimental data are required. It is customary to obtain these data under experimental conditions similar to those recommended by the American Vacuum Society,[5] which call for constant temperature and an experimental gas pressure low enough to be neglected, rendering the data pressure-independent. In lieu of appropriate experimental data, pressure dependence may be added to conventional data by introduction of an analytic pressure-dependent term. Rigorous derivation of such a term requires knowledge of the sorption isotherm for the system of interest and is outside the scope of the present paper. For the present purposes the experimental outgassing data have been fitted by an exponential series to obtain the following type of expression.

$$Q = \sum_{i=1}^{n} c_i \exp(k_i t) \tag{10}$$

Pressure dependence can be introduced to Eq. (10) as follows

$$Q = \left[\frac{P_0 - P}{P_0}\right] \sum_{i=1}^{n} c_i \exp(k_i t) \tag{11}$$

Here $P_0$ is the initial pressure of the system—usually one atmosphere—and $P$ is the instantaneous pressure during evacuation. The equation is correct at $P = P_0$ and $P \ll P_0$ and thus should represent a reasonable first-order approximation.

### *Comparison with experiments*

To evaluate the performance of the proposed analysis and to demonstrate its usefulness as a design tool, a comparison has been made of the experimentally measured and predicted evacuation pressure-histories of a laboratory scale-model multilayer insulation blanket. The experiment is described in detail in Ref. 6. The blanket consisted of alternate layers of crinkled double-aluminized Mylar shields and Tissuglas spacers. The 4-ft-wide blanket was wrapped on the longitudinal surface of a cylindrical tank whose circumference was about 4 ft. The diameter of the tank was large by comparison with the interlayer separation so the system was equivalent to the parallel plate model of Fig. 1. The length $2L$ was thus equal to 4 ft. The layer density was 76 shields/in. The cylindrical tank was 72 in. long and both its flat ends were independently insulated. The tank was placed inside a vacuum chamber and was fitted with capacitance manometers to measure both the absolute gas pressure in the vacuum chamber and the pressure differential between the insulation no-flow boundary and the vacuum chamber. The insulation was evacuated with the entire system at ambient temperature. Figure 2a shows the vacuum chamber pressure history, and Fig. 2b shows the measured pressure differential.

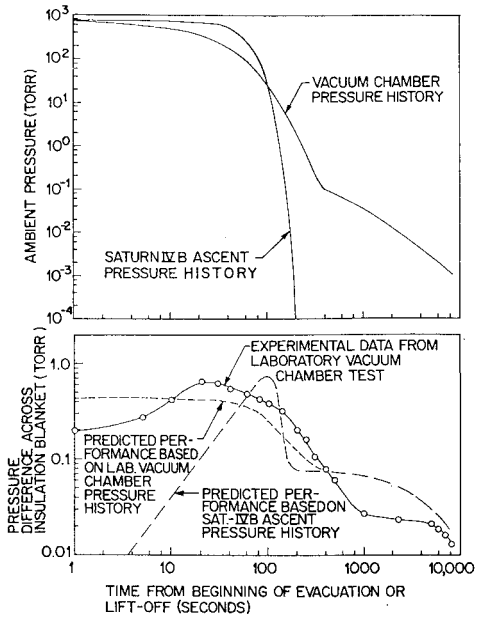


**Fig. 2 a) Pressure histories for the laboratory vacuum chamber and for a typical Saturn IVB stage ascent (top); b) measured and computed pressure differentials between the no-flow boundary and the ambient environment (bottom).**

The analysis presented in this paper was used to predict the experimentally measured pressure differentials. The flow equations given previously were solved using a numerical technique described by Schneider[7] for transient heat flow problems. The applied boundary conditions were

$$(\partial P_d/\partial x)_{x=0} = (\partial P_p/\partial x)_{x=0} = 0 \tag{12}$$

$$P_d(x,0) = 0 \text{ torr} \tag{13}$$

$$P_p(x,0) = 760 \text{ torr} \tag{14}$$

$$P_d(\pm L,t) + P_p(\pm L,t) = P_m(\pm L,t) \tag{15}$$

Equations (13) and (14) do not represent initial conditions in a wholly satisfactory manner. At $t = 0$ the partial pressure of the desorbing gas will be somewhere between zero and its normal vapor pressure. Solutions have been obtained with both these boundary conditions, and except at very early times no significant difference was found in the predicted values of differential pressure. $P_m(\pm L,t)$ was incorporated into the analysis in the form of a curve fit of the experimental chamber pressure history data from Fig. 2a. Outgassing data were included by curving-fitting experimental data for a crinkled double-aluminized Mylar-Tissuglas system[8] in as-received condition. The desorbed gas was assumed to be water vapor,[8] whereas the purge gas was helium. The computed pressure differential history is shown in Fig. 2b.

It can be seen from Fig. 2b that the general forms of the experimental and computed pressure differentials are similar in shape and magnitude. The experimental pressure history data of Ref. 6 were recorded after the insulation had been evacuated and repressurized with helium several times during checkout experiments. According to data presented in Ref. 8 this procedure can produce a permanent reduction in early-time outgassing rate of between 30% and 60%. This would be sufficient to produce the observed difference between computed and experimental figures. A rigorous evaluation of the analysis thus requires the use of outgassing data for insulation material processed in exactly the same manner as evacuation test insulation layup.

Using normal laboratory vacuum pumping apparatus and a constant volume chamber one obtains an approximately exponential pressure time history. The pressure history experienced by a launch vehicle differs in that the rate of ambient pressure decay will be very slow at first and then will rise rapidly to a very high value. Figure 2a shows a typical pressure history for a Saturn IVB stage. In order to demonstrate the difference in the pressure differentials induced by laboratory and launch ambient pressure histories the analysis was rerun using a curve fit to the Saturn IVB ambient pressure history to represent $P_m(L,t)$. The computed pressure differentials are shown in Fig. 2b. At long evacuation times they are identical to the laboratory case. At early times the shape of the curve is quite different, showing the pressure differential rising slowly to a maximum value almost twice that of the laboratory case and occurring at a later time.

The analytical solution was continued in time to determine when the interlayer gas pressure falls below $10^{-5}$ torr. Assuming ambient temperature and the Saturn IVB pressure history the analysis predicted that this would occur after about 30 hr of evacuation.

## Appendix: Derivation of Mean Gas Flow Velocity, $\bar{v}_x$

The mean gas flow velocity, $\bar{v}_x$, can be determined for flow in continuum transition and free molecule flow from a slip-flow modified laminar flow equation as follows. Reference is made to Fig. 1. The momentum equation for flow in the $x$ direction is

$$0 = \partial P/\partial x + \mu \partial^2 v_x/\partial y^2 \tag{A1}$$

Equation (A1) can be integrated in accordance with the boundary conditions

$$\partial v_x/\partial y = 0 \text{ at } y = 0,\ v_x = v_0 \text{ at } y = y_0$$

In pure laminar continuum flow $v_0$ is zero. In pure free molecule flow $v_0$ is equal to the velocity at the center line. In transition flow $v_0$ assumes some intermediate value. The following velocity distribution equation is obtained.

$$v_x = (-1/2\mu)[y_0^2 - y^2]\partial P/\partial x + v_0 \tag{A2}$$

The assumption is now made that the shear stress at the wall, $\tau$, is equal to a constant, $\varepsilon$, times the wall velocity, $v_0$. Since $\tau$ is by definition equal to $-\mu(\partial v_x/\partial y)$ at $y = y_0$, the following expression is obtained for $v_0$

$$v_0 = -(\mu/\varepsilon)(\partial v_x/\partial y)_{y=y_0} \tag{A3}$$

Equation (A2) can be integrated to find the average flow velocity $\bar{v}_x$, and $v_0$ can be replaced according to Eq. (A3) to give

$$\bar{v}_x = (-y_0^2/3\mu)[1 + 3\mu/\varepsilon y_0](\partial P/\partial x) \tag{A4}$$

The ratio $\mu/\varepsilon$ is known as the slip coefficient $\zeta$ and is given by (Ref. 4, p. 284)

$$\mu/\varepsilon = \zeta = (\mu/P) \cdot (\pi v_a/4)[(2-f)/f] \tag{A5}$$

$v_a$ is the mean molecular velocity given[9] by $v_a = (8R_0T/\pi M)^{1/2}$, $f$ is the specular reflection coefficient, and is the fraction of molecules incident upon the channel walls which are reflected diffusely. The value of $f$ must be determined experimentally, but it is usually slightly less than unity.[10] Substitution of these quantities in Eq. (A4) gives

$$\bar{v}_x = \frac{-y_0^2}{3\mu}\left[1 + \frac{3\mu}{y_0 P} \cdot \frac{\pi v_a}{4} \cdot \frac{2-f}{f}\right]\frac{\partial P}{\partial x} \tag{A6}$$

At high pressures the second term in the parentheses in Eq. (A6) becomes negligible and the familiar Poisseuille equation is obtained. At very low pressure free molecule flow will occur and this expression for $\bar{v}_x$ reduces to

$$\bar{v}_x = (-\pi/4)[(2-f)/f](y_0/P)v_a(\partial P/\partial x) \tag{A7}$$

The mass flow in the free molecule flow regime is governed by the Knudsen equation which, when rearranged, gives the average velocity as follows:

$$\bar{v}_x = -(4/3)(y_0/P)v_a(\partial P/\partial x) \quad \text{(A8)}$$

The constants in Eq. (A7) and (A8) agree if

$$\frac{4}{3} \equiv [(2-f)/f](\pi/4), \quad \text{or} \quad f \sim 0.75 \quad \text{(A9)}$$

This value of $f$ is somewhat lower than would be expected from experiment. By setting $f$ equal to this value in Eq. A6 the following expression for $\bar{v}_x$ is obtained.

$$\bar{v}_x = (-{y_0}^2/3\mu)[1 + (4\mu v_a/Py_0)](\partial P/\partial x) \quad \text{(A10)}$$

### References


[1] Nast, T. C. and Coston, R. M., "Investigation of the Gas Flow within Multilayer Insulations and its Effect on Cryogenic Space Vehicle Design," *Chemical Engineering Progress Symposium Series*, American Institute of Chemical Engineers, New York, Vol. 62. No. 61, 1966, pp. 184–192.

[2] Kneisel, K. M. and Benett, F. O., "Prediction of Interstitial Gas Pressure in a Multilayer Insulation during Rapid Evacuation," *Journal of Spacecraft and Rockets*, Vol. 7, No. 10, Oct. 1970, pp. 1259–1261.

[3] Gambill, W. E., "To Get Viscosity for a Gas Mixture," *Chemical Engineering*, Vol. 65, No. 23, Nov. 17, 1958, pp. 157–160.

[4] Loeb, L. B., *The Kinetic Theory of Gases*, 3rd ed. Dover, New York, 1961.

[5] "Reporting of Outgassing Data," Standard AVS-9, 1963. American Vacuum Society, Boston, Mass.

[6] Keller, C. W., "High Performance Thermal Protection Systems," Rept. LMSC A-964947, Dec. 1969, Lockheed Missile and Space Co., Sunnyvale, Calif., pp. 6.1–6.4.1.

[7] Schneider, P. J., *Conduction Heat Transfer*, 1st ed., Addison-Wesley, Reading, Mass., 1955, Chap. 12, p. 294.

[8] Glassford, A. P. M., "Outgassing Behavior of Multilayer Insulation Materials," *Journal Spacecraft and Rockets*, Vol. 7. No. 12, Dec. 1970, pp. 1464–1468.

[9] Dushiman, S., *Foundations of Vacuum Technique*, 2nd ed., Wiley, New York, 1962, Chap. 1, p. 9.

[10] Rohsenow, W. M. and Choi, H., *Heat Mass and Momentum Transfer*, 1st ed., Prentice-Hall, Englewood Cliffs, New Jersey, 1961, Chap. 11, p. 286.


# Dielectric Breakdown in a Dilute Plasma


D. J. McKinzie Jr.* and N. T. Grier†

*NASA Lewis Research Center, Cleveland, Ohio.*


### Introduction

RECENTLY, solar cell arrays operating at voltages up to 16 kv have been proposed as power sources in space. Array voltages in this range would be used to operate specialized electronic equipment without the need of a heavy power conditioning system. In 1968 R. K. Cole et al.[1] demonstrated the need for insulating such high voltage solar arrays from the electrically active plasma of the space environment at 500 km altitude. However, the effects of high voltage on desirable or candidate dielectrics are not well known and virtually no information is available on their breakdown voltages between a plasma and a metal electrode. Therefore, tests were made to determine these effects on the dielectrics now being considered for this application. The tests were performed at positive bias voltages as high as 20 kv d.c. relative to ground in an argon plasma with electron number densities of approximately $10^6$ particles per $cm^3$.


Received October 22, 1971; revision received December 20, 1971.

Index categories: Spacecraft Electric Power Systems; Properties of Materials; Radiation Protection Systems.



* Aerospace Engineer. Member AIAA.

† Aerospace Engineer.


### Apparatus and Procedure

*Facility*

The tests were performed in a 0.46 m diam by 0.76 m long Pyrex bell jar mounted in a side port of a 3.05 m diam by 4.57 m long vacuum tank (Fig. 1). The tank was operated at a vacuum condition of approximately $2 \times 10^{-5}$ torr. The test specimens were mounted on one end of a 3.2 cm diam cylindrical Pyrex sting. The ammeter used to detect dielectric breakdown and any leakage current preceding breakdown was located between the high voltage power supply and the test specimen. The wire connecting the test specimen, ammeter, and the power supply was shielded, with the shield at the potential of the test specimen. A 15-cm Kaufman ion thruster was used to generate the argon test plasma.

*Test Specimens*

The dielectrics tested are presented in Table 1. They are arranged in groups indicating their function in the design of a solar cell array (Fig. 2). Each specimen was positioned on the sting as shown in Fig. 3.

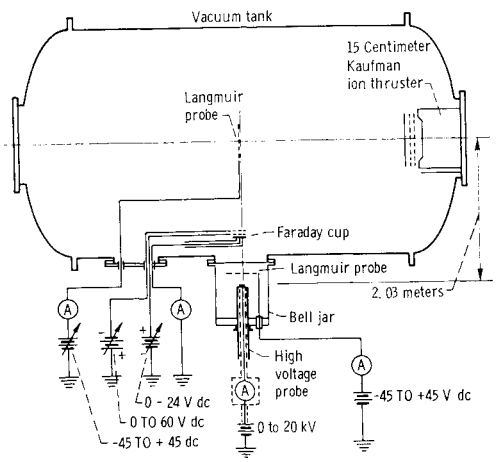


**Fig. 1 Sketch of experimental facility (not to scale).**

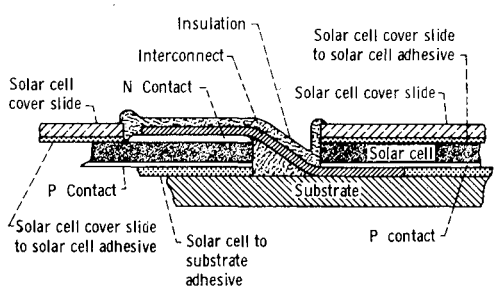


**Fig. 2 Cross-sectional view of insulated solar cell assembly showing dielectrics.**